the plant journal

SEB Society for Experimental Biology

The Plant Journal (2015) **81,** 493–504 doi: 10.1111/tpj.12745

The maize *brown midrib4* (*bm4)* gene encodes a functional folylpolyglutamate synthase

Li Li[1,2,†], Sarah Hill-Skinner[1], Sanzhen Liu[1,‡], Danielle Beuchle[3,§], Ho Man Tang[3,¶], Cheng-Ting Yeh[1], Dan Nettleton[4,5] and Patrick S. Schnable[1,3,4,*]

[1]*Department of Agronomy, Iowa State University, 2035 Roy J. Carver Co-Lab, Ames, IA 50011-3650, USA,*

[2]*College of Agronomy, Northwest Agriculture and Forestry University, #3, Taicheng road, Yangling, Shaanxi, 712100, China,*

[3]*Department of Genetics, Development and Cell Biology, Iowa State University, 1210 Molecular Biology Building, Ames, IA 50011-3260, USA,*

[4]*Center for Plant Genomics, Iowa State University, 2035 Roy J. Carver Co-Lab, Ames, IA 50011-3650, USA, and*

[5]*Department of Statistics, Iowa State University, 2115 Snedecor, Ames, IA 50011, USA.*

Received 10 September 2014; revised 3 December 2014; accepted 8 December 2014; published online 13 December 2014.

*For correspondence (e-mail schnable@iastate.edu).

Li Li and Sarah Hill-Skinner contributed equally to this work.

†Present address: Institute of Crop Sciences, Chinese Academy of Agricultural Sciences, Beijing 100081, China.

‡Present address: Department of Plant Pathology, Kansas State University, Manhattan, KS 66506, USA.

§Present address: Pioneer Hi-Bred International Inc., Johnston, IA 50131, USA.

¶Present address: Institute for Basic Biomedical Sciences, Johns Hopkins University School of Medicine, Baltimore, MD 21205, USA.

SUMMARY

Mutations in the *brown midrib4 (bm4)* gene affect the accumulation and composition of lignin in maize. Fine-mapping analysis of *bm4* narrowed the candidate region to an approximately 105 kb interval on chromosome 9 containing six genes. Only one of these six genes, GRMZM2G393334, showed decreased expression in mutants. At least four of 10 *Mu*-induced *bm4* mutant alleles contain a *Mu* insertion in the GRMZM2G393334 gene. Based on these results, we concluded that GRMZM2G393334 is the *bm4* gene. GRMZM2G393334 encodes a putative folylpolyglutamate synthase (FPGS), which functions in one-carbon (C1) metabolism to polyglutamylate substrates of folate-dependent enzymes. Yeast complementation experiments demonstrated that expression of the maize *bm4* gene in FPGS-deficient *met7* yeast is able to rescue the yeast mutant phenotype, thus demonstrating that *bm4* encodes a functional FPGS. Consistent with earlier studies, *bm4* mutants exhibit a modest decrease in lignin concentration and an overall increase in the S:G lignin ratio relative to wild-type. Orthologs of *bm4* include at least one paralogous gene in maize and various homologs in other grasses and dicots. Discovery of the gene underlying the *bm4* maize phenotype illustrates a role for FPGS in lignin biosynthesis.

Keywords: *brown midrib*, lignin, folylpolyglutamate synthase, folylpolyglutamate synthase, *Zea mays*, methylenetetrahydrofolate reductase.

INTRODUCTION

Maize *brown midrib* (*bm*) mutants, so named for the reddish-brown pigmentation of their midribs, affect lignin concentration and composition (Barriere *et al.*, 2004, 2007; Vermerris *et al.*, 2010). Lignin is a heteropolymer involved in the strengthening of stalks and contributes to the resistance of plants to some insects and pathogens (Santiago *et al.*, 2013). Lignin accumulates in the secondary cell walls and is cross-linked with arabinoxylans through ferulate bridges. In maize, polymers of lignin are composed of H, G, and S lignin, which, respectively, are composed of the three different hydroxycinnamoyl alcohol subunits (monolignols), p-coumaryl (H), coniferyl (G), and sinapyl (S) alcohol (Barriere *et al.*, 2007). Three of the six previously characterized *bm* mutants are known to be involved in the lignin biosynthetic pathway. *bm1* and *bm3* encode cinnamyl alcohol dehydrogenase (CAD) and caffeic acid *O*-methyltransferase (COMT), respectively. CAD catalyzes the synthesis of coniferyl and *p*-coumaryl alcohols, while

COMT catalyzes the synthesis of sinapyl alcohol (Vignols *et al.*, 1995; Halpin *et al.*, 1998). The recently cloned *bm2* encodes a functional methylenetetrahydrofolate reductase (MTHFR) involved in the formation of the key methyl donor, *S*-adenosyl-L-methionine (SAM) (Tang *et al.*, 2014). SAM links MTHFR with lignin biosynthesis by serving as a methyl donor for both COMT and caffeoyl CoA 3-*O*-methyltransferase (CCoAOMT) (Figure 1) (Tang *et al.*, 2014).

In this study, we describe the characterization and cloning of a fourth *bm* gene, *bm4*, which encodes a functional folylpolyglutamate synthase (FPGS, EC# 6.3.2.17) that acts upstream of MTHFR in the lignin biosynthetic pathway (Figure 1). FPGS functions in one-carbon (C1) metabolism to catalyze the γ-linked polyglutamylation of tetrahydrofolate (THF). In plants, C1 metabolism feeds into the biosynthesis of purines, thymidylate, serine, methionine, and formylmethionine (fMet) for which THF is required. Polyglutamylated folates are the preferred substrates of folate-dependent enzymes and are the principle forms of folate found in living cells (Cossins and Chen, 1997; Mehrshahi *et al.*, 2010). Thus, we hypothesize that FPGS-catalyzed polyglutamylation of THF stimulates the downstream synthesis of polyglutamylated 5-methyl THF catalyzed by the *bm2*-encoded MTHFR (Figure 1) (Tang *et al.*, 2014). It is therefore reasonable that a mutation in the FPGS gene (i.e., *bm4*) would alter lignin content and/or composition.

RESULTS

Mapping *bm4* to a 105 kb interval on chromosome 9

Like all *brown midrib* mutants, *bm4* mutants display a distinctive pigmentation phenotype relative to wild-type siblings (Figure 2b,g,i,k,m,o,q). The *bm4* mutation also affects the accumulation and composition of lignin (Table 1). These results suggested a role for *bm4* in lignin biosynthesis and provided the impetus to identify the gene underlying this mutant. Previously, the *bm4* gene had been mapped to the distal end of the long arm of chromosome 9 (Burnham, 1947). Our fine-mapping experiments (Experimental Procedures) established that the *bm4* gene is located in a 3 cM interval (198.5–201.2 cM) that encompasses physical positions 154.33–155.45 Mb of the maize reference genome (RefGen v2 [AGPv2] with gene annotations v5b.60). Subsequent mapping experiments narrowed the *bm4* candidate region to an approximately 127 kb interval (155 454–154 565 kb) that contains eight genes. A third mapping population consisting of 10 000 F_2 plants that was segregating for *bm4* was generated by selfing an F_1 derived from a cross between the inbred B73 and a mutant plant that carried *bm4-ref.* In this population, 1417 plants displayed the *bm4* phenotype (Tables S1 and S2). The shortage of mutant plants relative to the expected 25% is probably a consequence of an early-stage necrosis phenotype that co-segregates with the *bm4* phenotype in B73-derived populations segregating for *bm4-ref* (S. Hill-Skinner, unpublished observation). Because this necrotic phenotype was not observed in other populations segregating for *bm4* mutant alleles, there is no evidence to suggest that it is directly caused by *bm4* mutants. All *bm4* plants were screened for recombination events within subregions of the candidate interval (154.33–155.45 Mb, RefGen v2 [AGPv2] with gene annotations v5b.60) using PCR-based genotyping. Of the 56 identified recombinants, two were found to have recombination breakpoints within a 105 kb interval (154 397.6–154 502.6 kb). This interval contains six genes (Figure S1).

RNA-Seq analysis and gene expression of six candidate genes in the *bm4* fine-mapping interval

As part of a screen to determine whether any of the six genes in the candidate *bm4* interval were differentially expressed between *bm4* mutant and wild-type siblings, we conducted an unreplicated RNA-Seq experiment. Only one of these six genes showed significantly decreased expression based on Fisher's exact test (Figures S1 and S2B). This gene, GRMZM2G393334 (154 454 066–154 460 083 bp, RefGen v2 [AGPv2] with gene annotations v5b.60), encodes a putative FPGS. Because FPGS also has a substrate that is upstream of the *bm2*-encoded MTHFR enzyme (Figure 1) (Tang *et al.*, 2014), we selected GRMZM2G393334 as the *bm4* candidate gene.

The expression of GRMZM2G393334 across tissues of young seedlings and, to a lesser degree, mature plants was visualized via qTeller (qTeller.com) (Figure S3). Based on these results, GRMZM2G393334 is expressed in a wide variety of tissues as expected for an enzyme involved in a central metabolic process. In addition, quantitative reverse transcription polymerase chain reaction (qRT-PCR) of GRMZM2G393334 was performed on RNA extracted from plants each of which was homozygous for one of five *Mu*-derived *bm4* alleles or *bm4-ref* (Table S2). All the mutants accumulated less *bm4* transcript (2–16%) than the non-mutant B73 inbred (Figure 3), thereby confirming the results of the RNA-Seq analysis.

Seq-Walking based whole genome *Mu*-flanking sequencing

Seq-Walking (Li *et al.*, 2013) was conducted using DNA from *bm4* mutant plants isolated from six separate *Mu*-tagging events in 2011 (Methods) (Table S2). The rationale for this experiment is that at least some of these plants would be expected to contain *Mu* insertions in the *bm4* gene that are not present in non-mutant stocks. A Seq-Walking library was constructed from pooled DNA of all six *Mu* alleles. The library was sequenced using a Life Technologies' PGM instrument. A total of 296 304 out of 544 689 reads (54.4%) remained after quality trimming. Of these trimmed reads, 249 456 (84.2%) could be mapped to the B73 reference

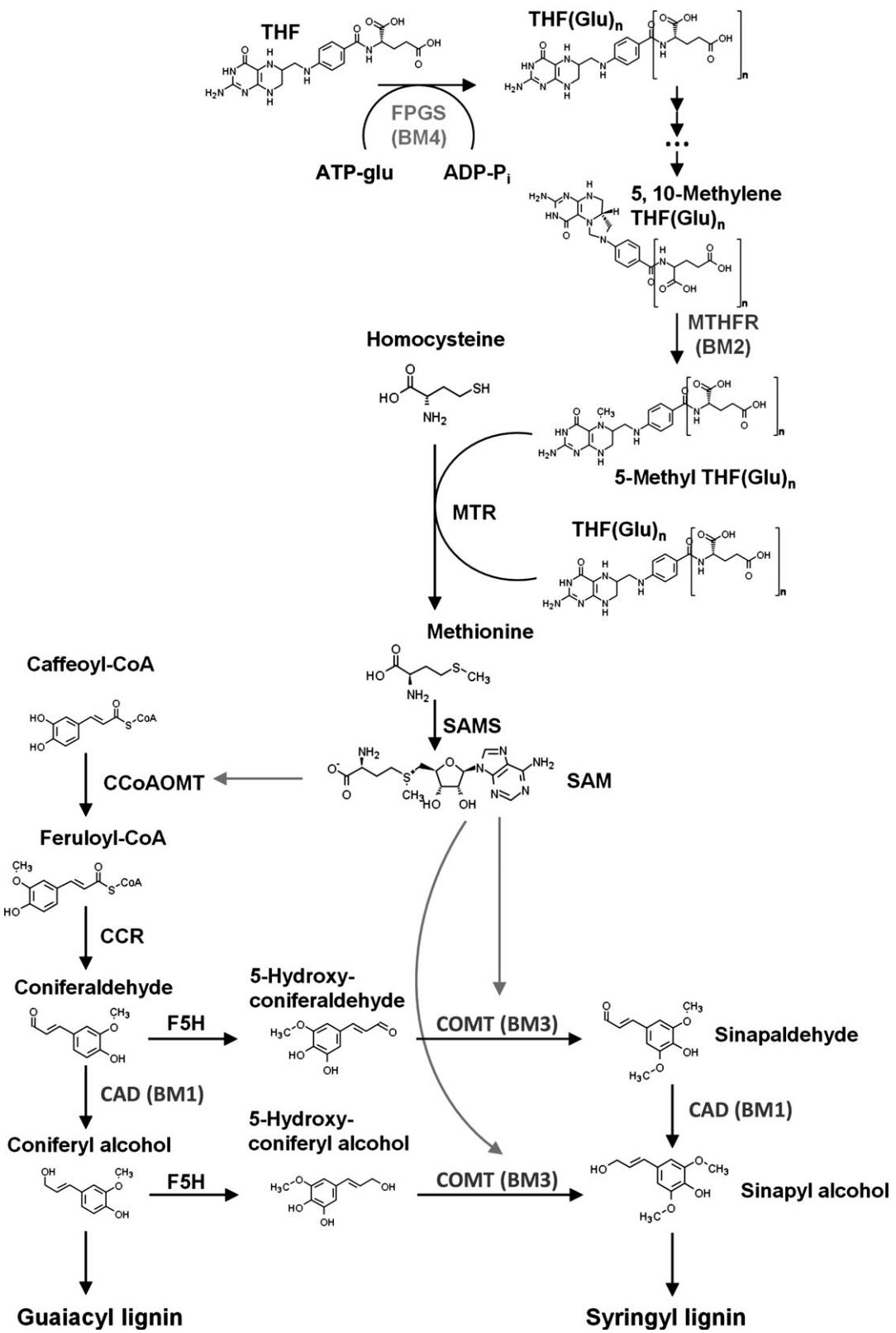

Figure 1. BM4 in connection with lignin biosynthesis.
FPGS (BM4) is connected to the lignin biosynthesis pathway through a series of polyglutamylated molecules and BM2. Chemical structures were downloaded from KEGG (http://www.genome.jp/kegg/). '…' indicates a series of steps that converts polyglutamylated THF to polyglutamylated 5,10-methylene THF (Cossins and Chen, 1997).

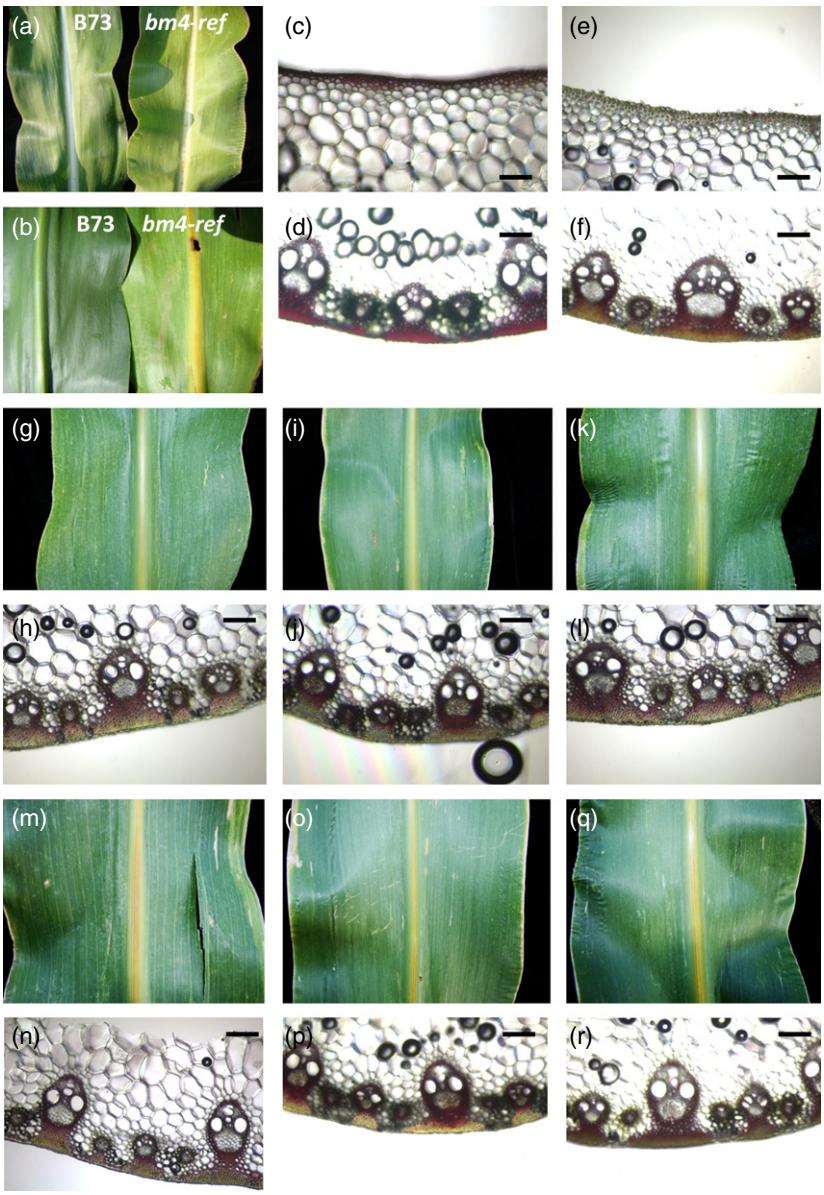

Figure 2. Phenotypic characterization of *bm4* mutant phenotypes.
bm4 mutants display reddish coloring of their leaf midribs. Plants shown were grown in the greenhouse under 27°C daytime temperature and 24°C night-time temperature.
(a, b) B73 wild-type and *bm4-ref*; (c, d) B73; (e, f) *bm4-ref*; (g, h) *bm4-Mu 13-7027D*; (i, j) *bm4-Mu 13-7029B*; (k, l) *bm4-Mu 13-7033E*; (m, n) *bm4-Mu 13-7064E*; (o, p) *bm4-Mu 11-8034B*; (q, r) *bm4-Mu 11-8050D*. Phenotypic appearance of the adaxial (a) and abaxial (b) sides of *bm4-ref* and B73 leaves. (g, i, k, m, o, q) Phenotypic appearance of the abaxial sides of *bm4-Mu* mutants. Phloroglucinol-hydrochloric acid staining of the adaxial (c) and abaxial (d) sides of B73 wild-type midrib tissue. Phloroglucinol-HCl staining of the adaxial (e) and abaxial (f, h, j, l, n, p, r) sides of *bm4* mutant midrib tissue. Scale bars = 100 μm.

genome and 238 118 (80.4%) could be uniquely aligned to the reference genome. In total, seven *Mu* insertions were detected within the *bm4* mapping interval in gene GRMZM2G393334 (Table S3). All but one of these insertion sites were represented by only a few reads (Table S3).

PCR-based sequencing of *Mu*-tagging alleles

To confirm the *Mu* insertions detected via Seq-Walking and determine which are associated with particular *bm4* mutant alleles, PCR primers were designed to amplify each insertion (Table S4). PCR was conducted on the original pre-pooled DNA samples used for Seq-Walking as well as DNA samples from the B73 inbred and a stock homozygous for the *bm4-ref* allele (Table S2). Strong PCR bands detected via gel electrophoresis were sequenced. These sequencing experiments confirmed the presence of a *Mu1* insertion in the first intron of the candidate gene for the plant carrying the *bm4-Mu 11-8050D* allele that was not detected in other DNA samples, including B73 and the *bm4-ref* stock (Figure 4).

Subsequently, similar PCR-based analyses were conducted on the four mutants isolated from the 2013 mutant screen using a series of gene-specific primers designed based on the sequence of GRMZM2G393334 in combination with the *Mu*TIR primer (Table S4 and Table S2). Allele-specific *Mu1* insertions were detected in exon 1, intron 2, and exon 4 of GRMZM2G393334 in the *bm4-Mu 13-7033E*, *bm4-Mu 13-7029B*, and *bm4-Mu 13-7064E* alleles, respectively (Figure 4). These results confirm that GRMZM2G 393334 is *bm4*.

Table 1 Lignin characteristics of wild-type and *bm4* mutant plants at different developmental stages

Year	Stage	Biological replicates (*n*)	Genotype	Klason lignin (g g^{-1} dry wt)	Klason difference |WT-MUT|	S/G	S/G difference |WT-MUT|	S (μmol g^{-1} dry wt)	G (μmol g^{-1} dry wt)	S + G (μmol g^{-1} dry wt)
2012	PA	1	WT	0.194 ± 0.011	0.027*	1.32	–	985	746	1731
			MUT	0.167 ± 0.005		1.50		966	646	1612
2010	PS	2	B73	0.245 ± 0.008	0.024*	1.62 ± 0.10	0.48	1274 ± 94	792 ± 108	2067 ± 202
			bm4-ref	0.221 ± 0.007		2.10 ± 0.27		1014 ± 147	482 ± 8	1496 ± 155
2012	PS	1	WT	0.198 ± 0.007	0.003	1.45	–	909	627	1535
			MUT	0.195 ± 0.004		2.06		715	347	1062
2014	PS	9	WT	0.252 ± 0.024	0.032*	1.72 ± 0.21	0.39*	1152 ± 355	689 ± 256	1841 ± 604
			MUT	0.220 ± 0.016		2.11 ± 0.14		868 ± 180	413 ± 89	1281 ± 266

Klason lignin values are based on 2–3 technical replicates. Compositional values are based on one technical replicate. One biological replicate is a single, whole stalk without leaves, ears, tassel, or roots.
MUT, mutant sibling homozygous for the *bm4-ref* allele; PA, post-anthesis (approximately 2-month-old); PS, post-senescence (approximately 5-month-old); WT, non-mutant, wild-type sibling.
*Significant difference based on a one-sided Student's *T*-test with significance level of $P < 0.05$.

Most of the GRMZM2G393334 gene, including the entire coding region, was amplified and sequenced from a stock homozygous for the *bm4-ref* allele. Sequence comparisons to the corresponding sequence from the B73 reference genome revealed 11 substitutions (three transversions and eight transitions), a single six-base insertion, and two single-base deletions in the coding region. Each of the 11 substitutions was also detected in at least one of the NAM founder inbreds (McMullen *et al.*, 2009), none of which display a *bm4* mutant phenotype, indicating that these substitutions are not the causal mutation of *bm4-ref.* Although the six-base insertion was not detected in the NAM founders, it was detected in three of four inbreds (Q66, Q67 and B77) that contributed to our *Mu*-active stocks (Dataset S2). The two deletions were detected in neither the NAM founder inbreds nor the *Mu* parents (Datasets S1 and S2). In particular, the deletion in exon 14 is predicted to cause a frameshift and premature stop codon in the translated protein (Figure S4). However, because non-coding regions of the gene which were not sequenced could harbor a causative mutation and the frameshift and premature stop codon would only affect the C-terminus of the protein which is in any case outside of the conserved domain it is not possible to conclude whether the deletions in the reference allele are causative.

To understand the origins of the six *bm4* mutants for which *Mu* insertions could not be identified, the *bm4* gene was amplified from DNA from mutant plants carrying these alleles. Based on the crossing strategy, these plants were expected to be heterozygous for a new *bm4* allele derived from the *Mu* parent and the *bm4-ref* allele. As discussed above, the *bm4-ref* allele contains at least 29 polymorphisms relative to the B73-derived *Bm4* allele (Datasets S1 and S2). Sequence analyses identified three substitutions in the coding region of the *bm4-Mu 11-8034B*/*bm4-ref* plant relative to the *bm4-ref* allele (Dataset S2), including a non-synonymous substitution in the conserved Mur_Ligase_M domain of GRMZM2G393334, which may have an impact on protein function (Figure S4). Because this substitution is not present in any of the 27 founder inbreds of the NAM population (McMullen *et al.*, 2009), it could potentially be causative. At all sites assayed, no polymorphisms were detected relative to *bm4-ref* in DNA from the other five *bm4-Mu* mutant plants, consistent with the hypothesis that these plants may carry maternally derived deletions of GRMZM2G393334, i.e. deletions that arose in the *Mu*-active stocks. Gene deletions have been identified previously from *Mu* stocks (Walbot, 2000).

bm4 encodes a functional FPGS

MET7 in yeast encodes an FPGS protein that is essential in methionine biosynthesis and *met7* mutant strains are methionine auxotrophs (Masselot and De Robichon-Szulmajster, 1975). Expression of maize *Bm4* (Figure S5) in

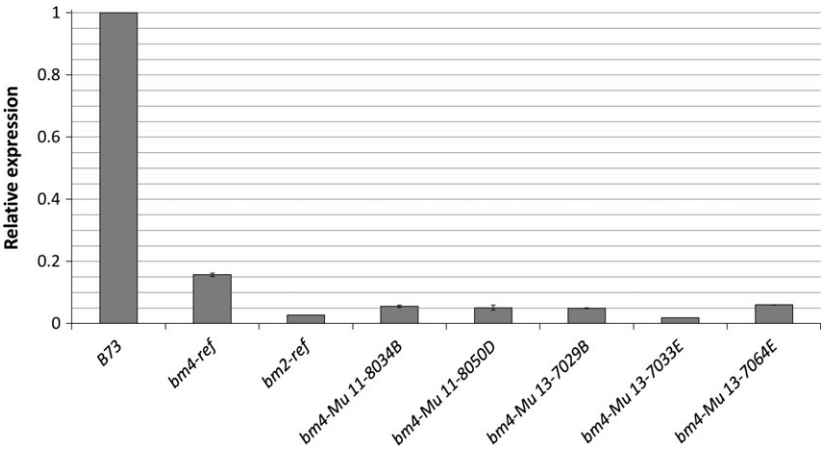

Figure 3. qRT-PCR expression analysis of *bm4-Mu* alleles.
The relative expression of *bm4* in *bm4-ref* mutants and five homozygous *bm4-Mu* mutants compared with B73 wild-type and the *bm2-ref* mutant (Tang *et al.*, 2014). Error bars indicate the standard error between technical replicates.

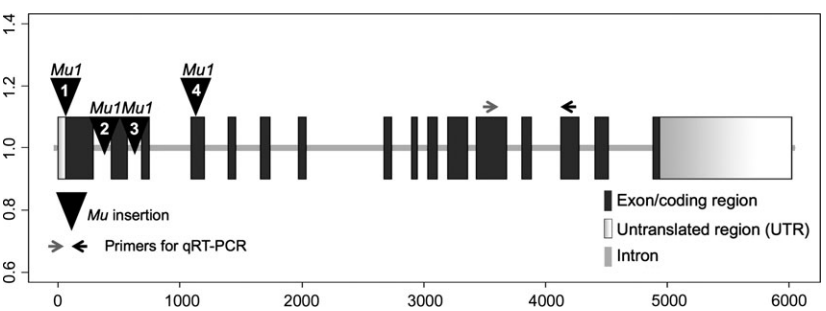

Figure 4. Sequence analysis of *bm4-Mu* alleles.
Mu insertions in *bm4* were detected in alleles: (1) *bm4-Mu 13-7033E*, (2) *bm4-Mu 11-8050D*, (3) *bm4-Mu 13-7029B*, and (4) *bm4-Mu 13-7064E*.

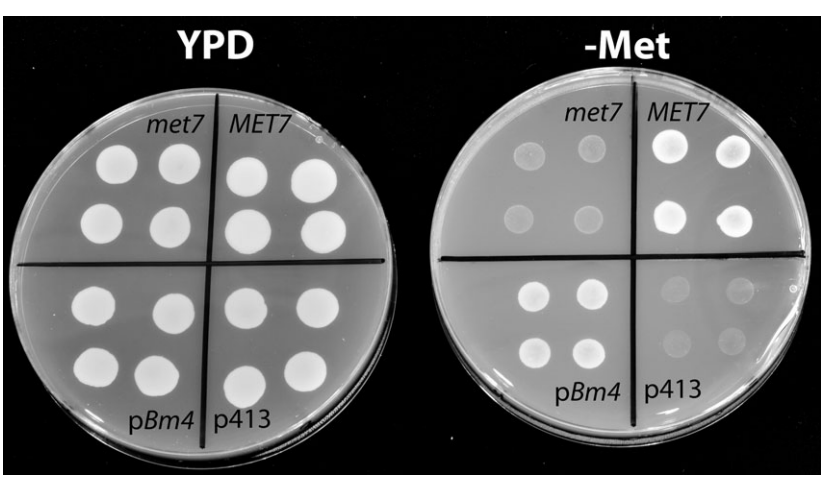

Figure 5. Maize-derived *Bm4* complements the yeast *met7* mutant phenotype.
met7 = untransformed haploid mutant *MATα met7* strain; *MET7* = untransformed haploid *MATα* non-mutant parent; p*Bm4* = *MATα met7* haploid mutant transformed with *Bm4*-containing p413-ADH shuttle vector; p413 = *MATα met7* haploid mutant transformed with empty p413-ADH shuttle vector. YPD = YPD media; −Me = SDC −Met medium.

mutant *MATα met7* strains successfully complemented the *met7* methionine auxotrophy (Figure 5), thus demonstrating that maize *bm4* encodes a functional FPGS.

bm4 lignin concentration and composition

Phloroglucinol–HCl staining reveals qualitative differences in lignin deposition in midrib tissues between *bm4* mutant lines and non-mutant controls (Vermerris *et al.*, 2010). Consistent with this previous study, we found that vascular tissue and epidermal cells of midribs from non-mutant plants (B73 in our case) stain much more heavily than do those of midribs of *bm4* mutant plants that are homozygous for the *bm4-ref* allele (Figure 2c–f). These results indicate greater deposition of lignin in B73 midribs. Similar differences were observed between B73 and plants that carried some of the newly isolated *bm4-Mu* alleles or that were putatively hemizygous (Figure 2h,j,l,n,p,r).

Lignin concentration and composition of stalks was measured quantitatively from plants that were backcrossed into B73 and homozygous for the *bm4-ref* allele and non-mutant controls. Lignin concentration and composition were determined using Klason lignin and thioacidolysis, as previously described (Tang *et al.*, 2014). Stalks were collected in 2010, 2012, and 2014. The 2010 experiment involved a comparison of *bm4-ref* mutants in a B73-like background (via two generations of backcrossing; Experimental Procedures) versus B73. These stalks were collected post-senescence (PS; approximately 5 months after planting). The 2012 and 2014 experiments involved comparisons of stalks from *bm4-ref* mutant and wild-type siblings, both of which were the products of three generations of backcrossing to B73. In the 2012 experiment, stalks were collected either post-anthesis (PA; approximately 2 months after planting) or PS from the same field. Stalks in the 2014 experiment were collected from the same field, but only PS. Probably as a consequence of the interest in using maize stover for animal feed, previous studies assayed lignin content in *brown midrib* mutants during the stage of development at which silage is harvested, i.e., after anthesis but before maturity (Barriere *et al.*, 2004; Vermerris *et al.*, 2010). Consistent with this prior literature, our analyses of lignin concentration revealed both PA and nearly all PS stalks assayed from plants homozygous for the *bm4-ref* allele accumulate approximately 10–14% less lignin than do wild-type siblings (Table 1) (Barriere *et al.*, 2004; Vermerris *et al.*, 2010). Similar to results obtained for *bm2* (Tang *et al.*, 2014), the ratio of S to G lignin is elevated in *bm4-ref* stalks relative to wild-type at both stages of development analyzed (Table 1).

Analysis of BM4 paralogs

BLASTP analysis of the protein sequence (AFW89831.1) encoded by the *bm4* gene (GRMZM2G393334) revealed at least one potential paralog in the maize genome. The GRMZM5G869779 gene encodes three protein isoforms (DAA49397.1, DAA49396.1, and DAA49398.1), which respectively share 72, 72, and 69% identity with BM4 over 93, 93, and 58% of the full-length BM4 sequence (Table S5). Like *bm4*, GRMZM5G869779 is expressed across many young, and to a lesser degree, mature tissues (Figure S6).

Analysis of BM4 homologs

As discussed above, the *bm4* gene encodes a functional FPGS. This enzyme has received significant attention because of its importance in human pathology (Galpin *et al.*, 1997; Rots *et al.*, 1999; Christoph *et al.*, 2012). In plants, FPGS is most often reported to be involved in the polyglutamylation of folates in C1 metabolism. These polyglutamylated folates are the preferred substrates of folate-dependent enzymes (Cossins and Chen, 1997; Mehrshahi *et al.*, 2010). Homologs of FPGS have been identified in various plant species. Among the grasses, FPGS proteins fall into two clades, the first of which contains the protein encoded by *bm4* (Figure 6 and Table S5). The *Oryza sativa*, *Brachypodium distachyon*, and *Setaria italica* protein sequences in the first clade share 86, 85, and 84% sequence identity with BM4 over 89, 89, and 100% of BM4, respectively. The *Sorghum bicolor*, *O. sativa*, *B. distachyon*, *S. italica*, and paralogous *Zea mays* (two isoforms) protein sequences in the second clade share 73, 70, 74, 73, and 72% sequence identity with BM4 over 89, 90, 94, 96, and 93% of BM4, respectively. The three FPGS genes of *Arabidopsis thaliana* share 50–62% sequence identity with BM4 (Figure 6 and Table S5). The proteins encoded by these three genes accumulate in the mitochondria, chloroplast, or cytosol, respectively (Ravanel *et al.*, 2001).

DISCUSSION

Six maize loci have been defined by *brown midrib* mutant phenotypes. Five of six of these mutants have shown to result in decreased lignin content of stalks (Halpin *et al.*, 1998; Barriere *et al.*, 2004, 2007; Guillaumie *et al.*, 2008; Vermerris *et al.*, 2010; Mechin *et al.*, 2014; Tang *et al.*, 2014). Three of these genes have been previously cloned

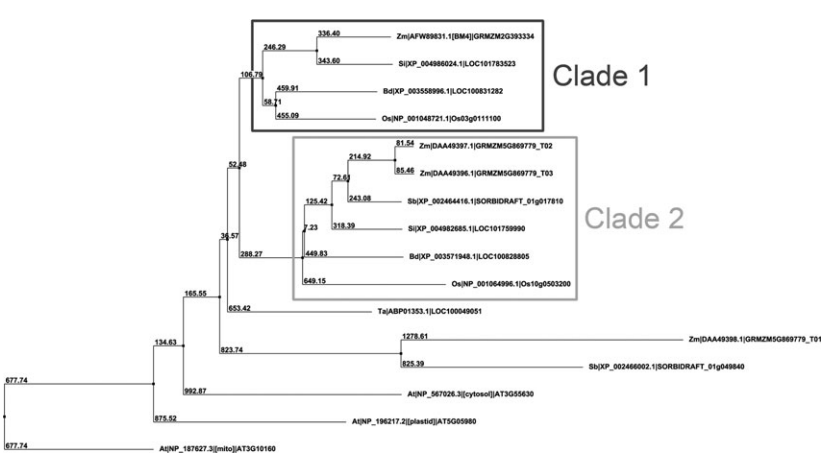

Figure 6. Homolog analysis of BM4.
Homolog analysis of BM4 across various plant species. 'I' separates the associated organism, Protein ID, and Gene ID of each protein sequence in the tree. The protein sequences used to construct the tree are the same as in Table S5. Brackets indicate either the name of the protein encoded or its subcellular localization. Boxes separate the two observed clades of FPGS proteins.

(*bm1*, *bm2*, and *bm3*) and each encodes a different lignin biosynthetic enzyme (Vignols *et al.*, 1995; Halpin *et al.*, 1998; Tang *et al.*, 2014). Lignin biosynthesis is important to plant growth and development because the cross-linking between lignin and other cell wall components via ferulate bridges limits solute transport across secondary cell walls and plays a role in increasing secondary cell wall rigidity and hence stalk strength (Santiago *et al.*, 2013). However, this cross-linking has adverse effects on ruminant digestion and biofuel production (Barriere *et al.*, 2007).

The *bm4* gene was cloned using physical mapping approaches in combination with Seq-Walking analysis of transposon-induced alleles. The physical interval defined by fine-mapping experiments contains six genes (Figure S1). Only one of these genes, GRMZM2G393334, showed significantly decreased expression in the *bm4-ref* mutant as compared with non-mutant siblings (Figures 3 and S2). PCR-based sequencing analyses of the entire protein-coding region identified numerous polymorphisms in the *bm4-ref* gene, including two deletions in the coding region that induce frameshifts and premature stop codons (Dataset S2 and Figure S4). However, without more in-depth analysis of the *bm4-ref* transcript, it remains unclear which of these or other mutations (perhaps in non-coding regions which were not sequenced) are causative. Seq-Walking experiments conducted on newly isolated *bm4-Mu* alleles identified *Mu* transposon insertions in GRMZM2G393334, establishing this gene as the *bm4* locus (Figure 4). Two of these *bm4-Mu* alleles carry a *Mu* insertion in an intron, a phenomenon that can also reduce gene expression level (Luehrsen and Walbot, 1992). It is of course also possible that the intronic *Mu* insertions could affect intron splicing. The *bm4* gene encodes a functional folylpolyglutamate synthase (FPGS) as demonstrated in yeast complementation experiments (Figure 5). FPGS is involved in the polyglutamylation of THF as part of one-carbon (C1) metabolism (Cossins and Chen, 1997; Mehrshahi *et al.*, 2010).

FPGS has been shown to play multiple roles in plants. The two known isoforms of FPGS of *Oryza sativa* appear to play roles in seed development (Anukul *et al.*, 2010). The three isoforms of FPGS of *Arabidopsis thaliana* accumulate in the mitochondria, chloroplast, and cytosol (Ravanel *et al.*, 2001). There is evidence that the mitochondrial FPGS is necessary for proper nitrogen utilization early in *Arabidopsis* seedling development (Jiang *et al.*, 2012). In addition, the plastidial FPGS is necessary for post-embryonic cell expansion and meristem maintenance in developing roots (Srivastava *et al.*, 2011). Double FPGS mutants in *Arabidopsis* have been shown to display embryo and seedling lethal phenotypes (Mehrshahi *et al.*, 2010). In contrast, our own studies show the maize *bm4* mutant does not exhibit any pronounced defects in seedling development, including roots (Figure S7).

We are unaware of any prior reports of FPGS affecting lignin biosynthesis. A role for this enzyme in this pathway is, however, consistent with the fact that polyglutamylated THF is converted by a series of steps to polyglutamylated 5,10-methylene THF, which is used by *bm2*-encoded MTHFR to generate 5-methyl THF (Cossins and Chen, 1997; Mehrshahi *et al.*, 2010). Polyglutamylated 5-methyl THF acts as a substrate for the synthesis of methionine, which is used as a substrate for the generation of SAM, which in turn serves as a methyl donor for the lignin biosynthetic enzymes COMT and CCoAOMT (Figure 1) (Tang *et al.*, 2014).

Consistent with the hypothesis that *bm4*-encoded FPGS works upstream of *bm2*-encoded MTHFR is the finding that both proteins are predicted to localize to the cytoplasm (Table S6). In addition, mutants in both genes display similar lignin phenotypes. Both mutants accumulate reduced concentrations of lignin in their stalks relative to wild-type. Notably, both mutants also exhibit increased ratios of S to G lignin in stalks relative to wild-type (Table 1) (Tang *et al.*, 2014). Finally, the *bm4* and *bm2* genes exhibit similar expression patterns across tissues (Figure S8). Vermerris *et al.* (2010) have reported that *bm2-bm4* double mutants exhibit further reductions in lignin accumulation relative to the single mutants and wild-type along with severe defects in plant growth. These studies were conducted using the reference alleles of *bm2* and *bm4.* The double mutant phenotype could be most easily explained if these reference alleles are leaky mutants, such that two partial defects in a common biochemical pathway would result in a more extreme phenotype than either partial defect alone. Our results indicate that the *bm4-ref* allele is leaky, but do not provide evidence for the *bm2-ref* allele being leaky (Figure 3).

Due to the involvement of FPGS in a key metabolic process, it was initially surprising that *bm4* mutant plants are viable even though they exhibit little *bm4* expression relative to non-mutants (Figure 3). We hypothesize that the *bm4* homolog GRMZM5G869779 provides sufficient FPGS activity to avoid lethality. Consistent with this hypothesis, GRMZM5G869779, like *bm4*, is expressed in many tissues (Figure S6).

In *Arabidopsis thaliana*, there are three known isoforms of FPGS. Each isoform is localized to the mitochondria, chloroplast, or cytosol. All forms act to polyglutamylate THF, but do so in a compartment-specific manner (Ravanel *et al.*, 2001). Polyglutamylation is thought to lock folates in the given compartment, thus directing them towards specific biosynthetic processes (Appling, 1991; Mehrshahi *et al.*, 2010). The putative cytosolic FPGS isoform is hypothesized to act upstream of the *bm2*-encoded MTHFR (Ravanel *et al.*, 2001). More recent literature suggests some functional overlap exists among the various *Arabidopsis* isoforms (Mehrshahi *et al.*, 2010). It is possible that the

maize FPGS isoforms behave in a similar fashion, because three of four subcellular localization predictions place BM4 in the cytoplasm (Table S6). However, subcellular localization of homologous FPGS proteins proved inconclusive. THF that is not polyglutamylated may diffuse into the cytosol and supply minimum levels of THF necessary for survival. Alternatively, the BM4 paralog may provide some baseline level of polyglutamylated THF to the pathway upstream of MTHFR. Other explanations may involve compensatory biochemical pathways. Due to the complex nature of carbon metabolism, it is possible that other yet discovered processes and enzymes may lead to polyglutamylated THF. The effect of *bm4* mutants on folate accumulation remains to be determined.

EXPERIMENTAL PROCEDURES

Phenotyping *bm4* mutants

Mutant *bm4* plants are easily distinguishable from non-mutants by the reddish-brown pigmentation of their leaf midribs (Figure 2b). This dark pigmentation is visible in leaf midribs approximately 1 month after planting and persists through maturity. This pigmentation is most obvious on the abaxial side of the leaf (Figure 2b,g,i,k,m,o,q).

Generation of *bm4 Mu*-tagged alleles

To assist in the identification of the *bm4* gene, new mutant alleles of *bm4* were isolated by screening large populations of plants derived from two separate crosses of *Mu*-active lines (female parents) by stocks homozygous for *bm4-ref* in 2011 (approximately 230 000 plants) and 2013 (approximately 138 000 plants), respectively. In combination, 10 F_1 plants that displayed the typical *bm4* phenotype (Figure 2b) were identified: six in the 2011 screen and four in the 2013 screen (Table S2).

Primer design

SNPs (single nucleotide polymorphisms) and Indel Polymorphisms (IDPs) for fine mapping the *bm4* gene were identified from RNA-Seq data (below). KASP primers to detect these SNPs were designed by LGC Genomics (www.lgcgenomics.com/). IDP primers and gene-specific primers were designed using the online primer design software, PRIMER 3 (http://biotools.umassmed.edu/bioapps/primer3_www.cgi).

bm4 fine mapping

The *bm4* gene was initially mapped on chromosome 9 to an interval (198.5–201.2 cM, 154.33–155.45 Mb, maize RefGen v2 [AGPv2] with gene annotations v5b.60) defined by the flanking Taqman probes SNPT3210 and SNPT6527 (Table S7), which were identified via comparisons between two genetic maps: MaizeGDB's IBM 2008 Neighbor 9 Map and ISU's IBM 2009 Integrated Map (Fu *et al.*, 2005; Lawrence *et al.*, 2008). Subsequently, fine mapping was conducted in 2009 using markers IDPbm4-4 and KASP000 (Table S7), which narrowed the mapping interval (154 438 813–154 565 293 bp, RefGen v2 [AGPv2] with gene annotations v5b.60) to one containing eight candidate genes. Additional fine-mapping experiments were conducted in 2013 using an F_2 population segregating for *bm4* and consisting of 10 000 plants derived from the cross between a plant that carried the *bm4-ref* mutant and the inbred line B73 (Table S2). Leaf tissue for DNA isolation was collected from 1417 mutant plants approximately 30 days after planting when the *bm4* phenotype (Figure 2b) could be scored. Recombinants in the mapping interval were identified using PCR-based IDP markers IDP154337900 and IDP154765138 (Table S7 and Table S1). Identified recombinants were then genotyped using various IDP and KASP markers within the mapping interval (Table S7 and Table S1).

RNA-Seq analysis

RNA-Seq was performed on an F_2 population of 200 plants segregating for *bm4* from a *bm4-ref* by B73 cross (Table S2). Plants were initially genotyped 21 days after planting and phenotyped 32–38 days after planting (Figure 2). Of the 200 plants, midrib tissue was collected from 50 genotyped *bm4-ref* mutants and 50 wild-type plants 41 days after planting. About 1 inch of tissue was collected from the second youngest leaf of each plant sampled and immediately frozen under liquid nitrogen. Midribs of the *bm4-ref* plants and wild-type plants were pooled separately and pools were ground under a stream of liquid nitrogen. RNA was extracted from the ground samples using Qiagen's RNeasy Plus Mini kit.

RNA-Seq libraries were prepared by the Iowa State University DNA Facility and sequenced using Illumina's GAII Sequencing technology. Single-end reads of length 75 bp were generated. After sequencing, raw reads were subjected to quality trimming according to the previously described method (Tang *et al.*, 2014). Fisher's exact test was used to test the null hypothesis that the proportions of reads of a given gene among the total reads in genic space are not different between the *bm4* mutants and wild-type siblings. Only genes with at least 40 total reads from both genotypes were used to perform Fisher's exact test. False discovery due to multiple testing was controlled (Benjamini and Hochberg, 1995). Genes with adjusted *P*-values (*q*-values) smaller than 0.001% and absolute value of $\log_2$ mutant/wild-type fold change > 1 were declared to be differentially expressed. Note that this comparison did not include biological replication. Both biological and technical variations could contribute to the differential expression between two samples. We, therefore, only used the results of this analysis in prioritizing candidate genes within the candidate interval.

Expression analysis using qTeller

The online tool qTeller (qTeller.com) was used to visualize the expression pattern of selected genes across various tissues. The data supplied by qTeller originates from RNA-Seq experiments conducted in various labs within the plant science community. Additional information on the datasets and in-house analysis can be found on the qTeller website: www.qteller.com.

qRT-PCR

One-month-old midribs from plants homozygous for five of the *bm4-Mu* alleles, *bm4-ref*, and B73 (Table S2) were collected according to the method described above for RNA-Seq analysis. Single pools of 3–4 midribs from separate plants were prepared for each genotype. RNA was extracted from each pool using Qiagen's RNeasy Plus Mini kit and reversed transcribed with Bio-Rad's iScript cDNA Synthesis kit. Thus, one cDNA library was prepared for each genotype. Two technical replicates of each cDNA sample were run with *bm4* gene-specific primers and two technical replicates of each cDNA sample were run with GAP primers. Quantitative real-time PCR was performed on a Roche Light Cycler 480II instrument using Bio-Rad's iQ SYBR Green Supermix.

Relative expression for each sample was quantified using the $2^{-\Delta\Delta Ct}$ method (Yuan *et al.*, 2006). A single expression value was calculated for each genotype by averaging across all technical replicates. *bm4* primers: (forward) bm4CE11L10.2 = 5′-TTGGCTAGTA CGTGGCTTGA-3′ and (reverse) bm4C1E12R10.1 = 5′-GCGCTCCAT CCAAATAAAAA-3′. GAP primers: (forward) gap987f = 5′-CTGAA CGACCACTTCGTCAA-3′ and (reverse) gap1143r = 5′-TTCTCGGCA TACACAAGCAG-3′.

Seq-Walking analysis

DNA from six heterozygous Mu-tagging lines (*bm4-Mu 11-8034B/bm4-ref*, *bm4-Mu 11-8050E-1/bm4-ref*, *bm4-Mu 11-8009D/bm4-ref*, *bm4-Mu 11-8050D/bm4-ref*, *bm4-Mu 11-8052B/bm4-ref*, and *bm4-Mu 11-8050E2/bm4-ref*) generated in 2011 from crosses between *bm4-ref* and *Mu*-active line plants was used for the Seq-Walking experiment (Li *et al.*, 2013) (Table S2). Pooled genomic DNA from these six lines was fragmented with a Diagenode Bioruptor sonicator at a frequency of 30 sec on/off. The fragmented DNA was then purified with a Qiagen Qiaquick PCR purification kit followed by Seq-Walking library preparation. Library preparation and data analysis was performed according to the previously published Seq-Walking method (Li *et al.*, 2013). Sequencing was performed using a Life Technologies' PGM instrument.

Validation of additional alleles via PCR and Sanger sequencing

All *bm4* alleles were additionally analyzed via PCR-based Sanger sequencing (Table S2). *Mu* alleles were sequenced from PCR products using a *Mu*-specific primer (*Mu*TIR: 5′-AGAGAAGCCAA CGCCA(AT)CGCCTC(CT)ATTTCGTC-3′) and *bm4* gene-specific primers (Table S4). A PCR product derived from the amplification of the *Mu*TIR primer and a primer designed from GRMZM2 G393334 (primer bm4C1E4R4.1) amplified in all DNA samples (Table S4). This PCR product is a false positive that is not associated with a *Mu* insertion. The entire transcribed regions of two of the alleles for which *Mu* insertions could not be identified (*bm4-Mu 11-8034B* and *bm4-Mu 13-7027D*) were sequenced using a combination of gene-specific primer pairs that covered the full-length of GRMZM2G393334 (Table S4). SEQUENCHER 5.1 software was used for sequence alignment. Protein domain analysis was performed with the online tool SMART. ClustalW alignment of *bm4* protein sequences was conducted using GenomeNet's Multiple Sequence Alignment by CLUSTALW tool.

Yeast complementation

The yeast *MAT*α *met7* mutant strain was selected for yeast complementation as *MET7* encodes an FPGS, which is essential for methionine synthesis (Masselot and De Robichon-Szulmajster, 1975). As such, *met7* yeast mutants are methionine auxotrophs and cannot grow on SDC –Met media. The *MAT*α *met7* mutant strain and *MAT*α non-mutant parental strain were purchased from GE Healthcare Dharmacon Inc. The complete *Bm4* coding sequence was synthesized using Integrated DNA Technologies' gene synthesis service. During synthesis, additional restriction sites were incorporated into the 5′ and 3′ regions of the *Bm4* coding sequence for use in cloning (Figure S5). Shuttle vector p413-ADH (Mumberg *et al.*, 1995), was obtained from ATCC. All vectors were transformed into and maintained in DH5α *E. coli* stocks cultured in LB medium containing 50 μg ml^{-1} ampicillin (Fisher,) and isolated via the alkaline lysis method (Sambrook and Russell, 2006). *E. coli* transformation was conducted via the $CaCl_2$ method (Mandel and Higa, 1970). Prior to cloning, both the shuttle vector and *Bm4* insert were digested using the restriction enzymes *Sal*I-HF and *Xba*I (New England BioLabs) following NEB's suggested conditions. The digested *Bm4* coding sequence and shuttle vector were isolated by gel electrophoresis using Bio-Rad Low Range Ultra Agarose and SYBR Gold (Life Technologies) and purified using Qiagen's Gel Purification Kit. Purified insert and vector were ligated using NEB's T4 DNA ligase following the manufacturer's recommended reaction conditions. *MAT*α *met7* mutant yeast were transformed with either cloned p413-ADH/*Bm4* vector or empty p413-ADH vector using the high-efficiency LiAc/SS Carrier DNA/PEG transformation method developed by the Gietz laboratory (http://home.cc.umanitoba.ca/~gietz/method.html) (Gietz and Woods, 2002). Gibco-BRL 10 mg ml^{-1} herring sperm DNA was used as the single-stranded carrier DNA. Transformants were selected for on SDC –His plates. Parental *MAT*α, untransformed *MAT*α *met7*, *MAT*α *met7* transformed with p413-ADH, and *MAT*α *met7* transformed with p413-ADH/*Bm4* strains were plated on YPD and SDC –Met media. SDC –His and –Met media were generated using Clontech –His and –Met/–Trp amino acid dropout media, respectively (http://www.clontech.com/). Other media ingredients used included Difco Bacto peptone, Bacto yeast extract, Bacto tryptone, Bacto agar, agar Noble, and yeast nitrogen base without amino acids. Additionally, Fisher dextrose, Acros LiAC dehydrate, and Sigma Trp and PEG3350 were also used. *MAT*α *met7*-derived yeast strains were cultured in media containing 200 μg ml^{-1} G418 (AdipoGen). All *E. coli* strains were incubated at 37°C for 1–2 days and all yeast strains were incubated at 30°C for 3–5 days.

Phloroglucinol–HCl staining

Midribs from 90-day-old *bm4* mutants and B73 plants were hand-sectioned and stained for approximately 1 min with phloroglucinol–HCl. Phloroglucinol–HCl was prepared as a 2:1 solution of 2% phloroglucinol in 95% ethanol and hydrochloric acid. Stained sections were viewed using a Nikon Eclipse E800 microscope with SPOT RT slider camera attachment (Diagnostic Instruments Inc.) and imaged using SPOT v. 4.0.6 software (Diagnostic Instruments Inc.).

Characterization of *bm4* lignin concentration and composition

Entire *bm4-ref* and wild-type stalks were collected for lignin analysis from field-grown F_2 plants derived from two-three successive rounds of backcrossing the *bm4-ref* allele into the B73 inbred. Stalks were collected either post-anthesis (PA; approximately 2 months after planting) or post-senescence (PS; approximately 5 months after planting). Stalks were cut at the first aboveground node and stripped of all leaves, ears, and tassels before air-drying for several weeks. Dried stalks were then processed through a Wiley mill with a 2 mm filter and the resulting stover was finely ground for 10 sec in a coffee grinder.

Approximately 300 mg of ground stover was analyzed for lignin concentration via Klason lignin as described previously (Tang *et al.*, 2014). The Klason lignin analyses from 2010, 2012, and 2014 are based on one, two, and nine biological replicates per genotype, respectively and three, three, and two technical replicates per sample, respectively. For lignin composition, 10 mg of stover was subjected to thioacidolysis and analyzed by GC-MS, also described previously (Tang *et al.*, 2014). The minor peaks associated with maize H-lignin are not detected using this method. Thioacidolysis analyses for 2010, 2012, and 2014 are based on one, two, and nine biological replicates per genotype, respectively. All thioacidolysis assays are based on one technical replicate per sample.

Identification of BM4 homologs

Homologs of maize BM4 were identified using NCBI's BLASTP algorithm with the full-length BM4 protein sequence. Homologs with E-values near zero were selected for inclusion in the FPGS phylogenetic tree, which was constructed using the free tool Jalview following the previously published method (Tang *et al*., 2014).

Subcellular localization

Subcellular localization predictions of proteins were conducted using online software PSORT, iPSORT, TARGETP, and MULTILOC2 (High-Res) separately with default parameters for plant analyses.

ACKNOWLEDGEMENTS

We thank the Schnable Laboratory nursery manager, Ms Lisa Coffey for generating and maintaining the genetic stocks and mutants used in this study, Drs Wei Wu and Yan Fu and Ms Mitzi Wilkening for assisting with the design of the first genetic mapping experiments, Dr An-Ping Hsia for helpful discussions, Drs Ann Perera and Zhihong Song of Iowa State University's W.M. Keck Metabolomics Research Laboratory for providing expertise in gas chromatography-mass spectrometry, Dr Alexis Campbell for providing her expertise in yeast transformation, Life Technologies for providing sequencing reagents, and Mike Baker of Iowa State University's DNA facility for providing instrument access.

CONFLICT OF INTEREST

The authors have no conflict of interest to report.

SUPPORTING INFORMATION

Additional Supporting Information may be found in the online version of this article.

Figure S1. Fine mapping indicates *bm4* is located in a 105 kb interval.

Figure S2. RNA-Seq expression of 6 genes in the *bm4* fine mapping interval.

Figure S3. qTeller results for *bm4* gene expression across different maize tissue types.

Figure S4. Amino acid and conserved domain analysis of *bm4* alleles *bm4-ref* and *bm4-Mu 11-8034B.*

Figure S5. *Bm4* sequence design for yeast complementation.

Figure S6. Expression pattern of *bm4* versus expression pattern of paralog GRMZM5G869779.

Figure S7. Comparison of *bm4-ref* and B73 seedling roots.

Figure S8. Expression pattern of *bm4* versus expression pattern of *bm2.*

Table S1. *bm4* fine mapping scores.

Table S2. Summary of *bm4* alleles.

Table S3. Seq-Walking targets in the *bm4* fine mapping interval.

Table S4. Primer information for *bm4* sequence and qRT-PCR analyses.

Table S5. Homologs of BM4.

Table S6. Subcellular localization prediction for BM4 and protein homologs in other grasses.

Table S7. Markers used for *bm4* fine mapping.

Dataset S1. SNP information for the *bm4* gene across various lines.

Dataset S2. SNP information for *bm4-Mu* alleles and their progenitors.

REFERENCES

Anukul, N., Ramos, R.A., Mehrshahi, P., Castelazo, A.S., Parker, H., Diévart, A. and Bennett, M.J. (2010) Folate polyglutamylation is required for rice seed development. *Rice*, **3**, 181–193.

Appling, D.R. (1991) Compartmentation of folate-mediated one-carbon metabolism in eukaryotes. *FASEB*, **5**, 2645–2651.

Barriere, Y., Ralph, J., Mechin, V., Guillaumie, S., Grabber, J.H., Argillier, O., Chabbert, B. and Lapierre, C. (2004) Genetic and molecular basis of grass cell wall biosynthesis and degradability. II. Lessons from *brown midrib* mutants. *C.R. Biol.* **327**, 847–860.

Barriere, Y., Riboulet, C., Mechin, V., Maltese, S., Pichon, M., Cardinal, A., Lapierre, C., Lubberstedt, T. and Martinant, J.-P. (2007) Genetics and genomics of lignification in grass cell walls based on maize as model species. *Genes Genomes Genomics*, **1**, 133–156.

Benjamini, Y. and Hochberg, Y. (1995) Controlling the false discovery rate: a practical and powerful approach to multiple testing. *J. R. Stat. Soc. Series B Stat. Methodol.* **57**, 289–300.

Burnham, C.R. (1947) Chromosome disjunction. *Maize Genet. Coop. Newsletter*, **21**, 36–37.

Christoph, D.C., Asuncion, B.R., Mascaux, C., Tran, C., Lu, X., Wynes, M.W. and Hirsch, F.R. (2012) Folylpoly-glutamate synthetase expression is associated with tumor response and outcome from pemetrexed-based chemotherapy in malignant pleural mesothelioma. *J. Thorac. Oncol.* **7**, 1440–1448.

Cossins, E.A. and Chen, L. (1997) Folates and one-carbon metabolism in plants and fungi. *Phytochemistry*, **45**, 437–452.

Fu, Y., Emrich, S.J., Guo, L., Wen, T.J., Ashlock, D.A., Aluru, S. and Schnable, P.S. (2005) Quality assessment of maize assembled genomic islands (MAGIs) and large-scale experimental verification of predicted genes. *Proc. Natl Acad. Sci. USA*, **102**, 12282–12287.

Galpin, A.J., Schuetz, J.D., Masson, E., Yanishevski, Y., Synold, T.W., Barredo, J.C. and Evans, W.E. (1997) Differences in folylpolyglutamate synthetase and dihydrofolate reductase expression in human B-lineage versus T-lineage leukemic lymphoblasts: mechanisms for lineage differences in methotrexate polyglutamylation and cytotoxicity. *Mol. Pharmacol.* **52**, 155–163.

Gietz, R.D. and Woods, R.A. (2002) Transformation of yeast by lithium acetate/single-stranded carrier DNA/polyethylene glycol method. *Methods Enzymol.* **350**, 87–96.

Guillaumie, S., Goffner, D., Barbier, O., Martinant, J., Pichon, M. and Barriere, Y. (2008) Expression of cell wall related genes in basal and ear internodes of silking *brown-midrib-3*, caffeic acid O-methyltransferase (COMT) down-regulated, and normal maize plants. *BMC Plant Biol.* **8**, 71.

Halpin, C., Holt, K., Chojecki, J., Oliver, D., Chabbert, B., Monties, B. and Foxon, G.A. (1998) *Brown) C.*, maize (*bm1*)-a mutation affecting the cinnamyl alcohol dehydrogenase gene. *Plant J.* **14**, 545–553.

Jiang, L., Liu, Y., Sun, H. *et al.* (2012) The mitochondrial folylpolyglutamate synthetase gene is required for nitrogen utilization during early seedling development in *Arabidopsis*. *Plant Physiol.* **161**, 971–989.

Lawrence, C.J., Harper, L.C., Schaeffer, M.L., Sen, T.Z., Seigfried, T.E. and Campbell, D.A. (2008) MaizeGDB: the maize model organism database for basic, translational, and applied research. *Int. J. Plant Genomics*, **2008**, 496957.

Li, L., Li, D., Liu, S. *et al.* (2013) The maize *glossy13* gene, cloned via BSR-Seq and Seq-Walking encodes a putative ABC transporter required for the normal accumulation of epicuticular waxes. *PLoS One*, **8**, e82333.

Luehrsen, K.R. and Walbot, V. (1992) Insertion of non-intron sequence into maize introns interferes with splicing. *Nucleic Acids Res.* **20**, 5181–5187.

Mandel, M. and Higa, A. (1970) Calcium-dependent bacteriophage DNA infection. *J. Mol. Biol.* **53**, 159–162.

Masselot, M. and De Robichon-Szulmajster, H. (1975) Methionine biosynthesis in *Saccharomyces cerevisiae.* I. Genetical analysis of auxotrophic mutants. *Mol. Gen. Genet.* **139**, 121–132.

McMullen, M.D., Kresovich, S., Villeda, H.S., Bradbury, P., Li, H., Sun, Q. and Buckler, E.S. (2009) Genetic properties of the maize nested association mapping population. *Science*, **325**, 737–740.

Mechin, V., Laluc, A., Legee, F., Laurent, C., Denoue, D., Barriere, Y. and Lapierre, C. (2014) Impact of the *brown-midrib bm5* mutation on maize lignins. *J. Agric. Food Chem.* **62**, 5102–5107.

Mehrshahi, P., Gonzalez-Jorge, S., Akhtar, T.A. *et al.* (2010) Functional analysis of folate polyglutamylation and its essential role in plant metabolism and development. *Plant J.* **64**, 267–279.

Mumberg, D., Muller, R. and Funk, M. (1995) Yeast vectors for the controlled expression of heterologous proteins in different genetic backgrounds. *Gene*, **156**, 119–122.

Ravanel, S., Cherest, H., Jabrin, S., Grunwald, D., Surdin-Kerjan, Y., Douce, R. and Rébeillé, F. (2001) Tetrahydrofolate biosynthesis in plants: molecular and functional characterization of dihydrofolate synthetase and three isoforms of folylpolyglutamate synthetase in *Arabidopsis thaliana*. *Proc. Natl Acad. Sci. USA*, **98**, 15360–15365.

Rots, M.G., Pieters, R., Peters, G.J., Noordhuis, P., van Zantwijk, C.H., Kaspers, G.J. and Jansen, G. (1999) Role of folylpolyglutamate synthetase and folylpolyglutamate hydrolase in methotrexate accumulation and polyglutamylation in childhood leukemia. *Blood*, **93**, 1677–1683.

Sambrook, J. and Russell, D.W. (2006) Preparation of plasmid DNA by alkaline lysis with SDS: minipreparation. *Cold Spring Harb. Protoc.* **1**.

Santiago, B., Barros-Rios, J. and Malvar, R.A. (2013) Impact of cell wall composition on maize resistance to pests and diseases. *Int. J. Mol. Sci.* **14**, 6960–6980.

Srivastava, A.C., Ramos-Parra, P.A., Bedair, M., Robledo-Hernández, A.L., Tang, Y., Sumner, L.W. and Blancaflor, E.B. (2011) The folylpolyglutamate synthetase plastidial isoform is required for postembryonic root development in *Arabidopsis*. *Plant Physiol.* **155**, 1237–1251.

Tang, H.M., Liu, S., Hill-Skinner, S., Wu, W., Reed, D., Yeh, C.T., Nettleton, D. and Schnable, P.S. (2014) The *maize brown midrib2 (bm2)* gene encodes a methylenetetrahydrofolate reductase that contributes to lignin accumulation. *Plant J.* **77**, 380–392.

Vermerris, W., Sherman, D.M. and McIntrye, L.M. (2010) Phenotypic plasticity in cell walls of maize *brown midrib* mutants is limited by lignin composition. *J. Exp. Bot.* **61**, 2479–2490.

Vignols, F., Rigau, J., Torres, M.A., Capellades, M. and Puigdomènech, P. (1995) The *brown midrib3 (bm3)* mutation in maize occurs in the gene encoding caffeic acid O-methyltransferase. *Plant Cell*, **4**, 407–416.

Walbot, V. (2000) Saturation mutagenesis using maize transposons. *Curr. Opin. Plant Biol.* **3**, 103–107.

Yuan, J.S., Reed, A., Chen, F. and Stewart, C.N. (2006) Statistical analysis of real-time PCR data. *BMC Bioinformatics*, **7**, 85.